Carbon Isotopic Evidence for Methane Hydrate Instability During Quaternary Interstadials

James P. Kennett, *et al.*

Science **288**, 128 (2000);
DOI: 10.1126/science.288.5463.128

Science (print ISSN 0036-8075; online ISSN 1095-9203) is published weekly, except the last week in December, by the American Association for the Advancement of Science, 1200 New York Avenue NW, Washington, DC 20005.

packed in a polypropylene column (0.5 cm^2 × 3.7 cm). Fe was entirely eluted with ~8 ml of 2 M HCl + 0.001% H_2O_2, flowing at a rate of ~0.3 ml/min. The eluate was collected in a series of fractions, ranging in size from 0.2 to 2 ml. Elution fractions were dried and redissolved in 1 ml of 0.05 M HNO_3. About 20% of each solution was used to determine Fe concentrations by ultraviolet–visible light spectrophotometry. The remainder was diluted to a concentration of ~3 parts per million Fe for isotopic analysis. All experiments were conducted in a clean lab with acid-cleaned Teflon labware, acid-cleaned resin, and ultrapure reagents.

16. T. I. Taylor and H. C. Urey, *J. Chem. Phys.* **6**, 429 (1938).
17. W. A. Russell and D. A. Papanastassiou, *Anal. Chem.* **50**, 1151 (1978).
18. E. Glueckauf, *Trans. Faraday Soc.* **54**, 1203 (1956).
19. T. N. van der Walt *et al.*, *Solvent Extr. Ion Exch.* **3**, 723 (1985).
20. K. W. Mandernack, D. A. Bazylinski, W. C. Shanks III, T. D. Bullen, *Science* **285**, 1892 (1999).
21. R. E. Criss, *Principles of Stable Isotope Distribution* (Oxford Univ. Press, New York, 1999).
22. These values should be regarded as order-of-magnitude estimates because this treatment is strictly valid only when the number of theoretical plates $>10^3$ (*18*). However, it has been shown to be a reasonable approximation for smaller columns (*17*). In addition, although kinetic effects may either attenuate or amplify isotopic separation, equilibration with ion-exchange resins is generally rapid on the time scales in our experiments, and the kinetics of equilibration between Fe(III) and AG MP-1 resin are at least as rapid as with other anion exchangers (*19*). The kinetics of Fe(III) ligand exchange are also rapid.
23. J. Bigeleisen and M. G. Mayer, *J. Chem. Phys.* **15**, 261 (1947).
24. M. Magini and T. Radnai, *J. Chem. Phys.* **71**, 4255 (1979).
25. M. J. Apted *et al.*, *Geochim. Cosmochim. Acta* **49**, 2081 (1985).
26. J. B. Neilands, *J. Biol. Chem.* **270**, 26723 (1995).
27. T. D. Bullen *et al.*, *Eos* **80**, 479 (1999).
28. From an ideal Gaussian elution curve, *N*, the number of theoretical plates in the column, is readily obtained from the relation $N = 5.57 \times (v_R/W_{1/2})^2$, where v_R is the volume to the curve peak and $W_{1/2}$ is the width of the curve at half-height (*14*). Here, if we neglect tailing, $N \sim 250$.
29. We thank F. Albarède, M. Anbar, B. Beard, R. Eisenberg, D. Farnsworth, J. Hayes, C. Johnson, J. Morgan, G. Ravizza, G. Rossman, E. Schauble, and G. Wasserburg for discussions. This research was conducted at the ICP-MS Laboratory of the University of Rochester, with support from NSF (EAR 9601929 and CHE 9714282) and the NASA Astrobiology Institute.

18 November 1999; accepted 24 February 2000

Carbon Isotopic Evidence for Methane Hydrate Instability During Quaternary Interstadials

James P. Kennett,[1]* Kevin G. Cannariato,[1] Ingrid L. Hendy,[1] Richard J. Behl[2]

Large (about 5 per mil) millennial-scale benthic foraminiferal carbon isotopic oscillations in the Santa Barbara Basin during the last 60,000 years reflect widespread shoaling of sedimentary methane gradients and increased outgassing from gas hydrate dissociation during interstadials. Furthermore, several large, brief, negative excursions (up to –6 per mil) coinciding with smaller shifts (up to –3 per mil) in depth-stratified planktonic foraminiferal species indicate massive releases of methane from basin sediments. Gas hydrate stability was modulated by intermediate-water temperature changes induced by switches in thermohaline circulation. These oscillations were likely widespread along the California margin and elsewhere, affecting gas hydrate instability and contributing to millennial-scale atmospheric methane oscillations.

Polar ice cores document large oscillations in atmospheric methane (CH_4) associated with Quaternary climate cycles on orbital, millennial, and decadal time scales (*1, 2*). Dramatic warmings during the first few decades of interglacials and interstadials coincided with rapid atmospheric CH_4 increases (*3*). These rises in CH_4 have been attributed to, in one hypothesis, enhanced methanogenesis in tropical wetlands receiving greater precipitation (*1–3*). However, extensive wetlands (*4*) are unlikely to have developed fast enough during sea-level low stands to account for the rapid rate of increase of atmospheric CH_4.

Another potential source of atmospheric CH_4 is methane (gas) hydrate, a solid formed in sediments from water and CH_4 under conditions of high pressure, low temperature, and sufficient gas concentrations (*5*). Large amounts of CH_4 (1×10^{19} to 2×10^{19} g) are stored on continental margins as gas hydrate and free gas trapped beneath (*6*). The majority of this CH_4 has very negative carbon isotopic values [~−65 per mil (‰)] typical for biogenic CH_4 produced by methanogenesis within anoxic sediments (*7*). The depth zone over which hydrates remain stable is dependent on water depth (pressure) and temperature (*8*). Gas hydrate dissociation can result from pressure decrease due to sea-level fall (*9*) or water temperature increase, the latter of which has been suggested for the late Paleocene (*10*) and observed on a small scale in the Gulf of Mexico (*11*). Released CH_4 is transferred to the exchangeable carbon reservoir by diffusion into the water column or by ebullition into the atmosphere as a result of sediment slope failure, sliding, or collapse (*10*).

Little is known about the stability of continental margin gas hydrates during the Quaternary. Decomposition of gas hydrates destabilizes the sediment column by creating abnormally high porosity at depth (*5*). Widespread sediment disruption (slumps, slides, pockmarks) on upper continental margins represents evidence for major CH_4 release from the ocean floor during the late Quaternary (*5, 12, 13*). The extent of this evidence reflects the magnitude of past release of ocean floor CH_4 and its potential to influence climate change. Several workers have attributed gas hydrate dissociation on the continental margins to sea-level fall during the Quaternary (*9*). However, temperature change has not been implicated previously as a potential factor in Quaternary gas hydrate stability, because there has been little previous evidence for Quaternary temperature increases of sufficient magnitude in upper intermediate-waters (400 to 1000 m) (*14*). Indeed, a seafloor source for CH_4 in ice cores has been dismissed, because inferred increases in atmospheric concentrations occurred during warm intervals when sea level, and hence hydrostatic pressure, was higher (*2*). Nevertheless, strong evidence exists for the role of temperature change, related to deep-sea thermohaline circulation switching, in gas hydrate dissociation during the late Paleocene thermal maximum (*10*).

Recent paleoclimatic records from the California margin exhibit the complete sequence of millennial-scale climate oscillations, termed Dansgaard-Oeschger (D-O) cycles, during the last 60 thousand years (kyr) (*15–17*). These are reflected as sea-surface temperature (SST) changes (*16, 17*), linked via the atmosphere with Greenland climate change (*18*), bottom-water oxygenation as indicated by lamination strength (*15*) and benthic foraminiferal assemblages (*15, 19*), and bottom-water temperatures (*16, 20*). Oxygenation switches on the continental margin resulted from changes in intermediate-water ventilation and surface-water productivity related to thermohaline circulation switches (*15, 16, 19–21*).

Here, we present high-resolution planktonic and benthic foraminiferal carbon and

[1]Geological Sciences and Marine Science Institute, University of California, Santa Barbara, CA 93106, USA. [2]Department of Geological Sciences, California State University, Long Beach, CA 90840, USA.

*To whom correspondence should be addressed. E-mail: kennett@geology.ucsb.edu

oxygen isotopic records for the last 60 kyr (*22*) from Ocean Drilling Program (ODP) Hole 893A, Santa Barbara Basin (34°17.25′N, 120°02.20′W; 580 m water depth) (Fig. 1) (*23*). This core, the highest resolution marine sequence known for the late Quaternary (*23, 17*), provides an unprecedented window through which past submillennial climate and oceanographic change can be viewed. We propose that intermediate-water temperature changes associated with D-O cycles modulated CH_4 outgassing and episodic massive gas hydrate dissociation in the depth zone of potential gas hydrate instability (*24*). This process may have occurred over broad regions and contributed to atmospheric CH_4 oscillations. Present-day gas hydrates are known to exist at water depths of potential gas hydrate instability (zone between ~400 and 1000 m in which gas hydrates can be destabilized by changes in bottom-water temperature and/or sea level) on the California continental margin (Fig. 1). Increasing geological evidence exists for widespread instability in the recent past (*25*). Santa Barbara Basin sediments today contain abundant CH_4 and shallow (~30 to 50 m subsurface) bottom-simulating reflectors, which are interpreted to be gas hydrates (*26*).

The late Quaternary submillennial climatic oscillations recorded by planktonic $\delta^{18}O$ values in Hole 893A (*17*) are associated with alternations in sediment lamination and benthic foraminiferal oxygen and carbon isotopic ratios (expressed as $\delta^{18}O$ and $\delta^{13}C$), reflecting large changes in ventilation, within the silled basin (Figs. 2 and 3). The planktonic foraminiferal $\delta^{18}O$ (*17*) and assemblage records (*27*) document a complete sequence of D-O cycles (interstadials 17 to 1), the Younger Dryas, and the Holocene epoch (Fig. 2) (*16*). Benthic $\delta^{18}O$ values also oscillate in concert with D-O cycles (Fig. 2); bottom-water temperatures were warmer during interstadials and cooler during stadials, with rapid changes occurring at the transitions (*20*). Decreases in benthic $\delta^{18}O$ values almost always preceded (up to 200 years) interstadial beginnings, as marked by rapid changes in planktonic foraminiferal assemblages and decreased planktonic $\delta^{18}O$ values (*20*). Thus, warming of intermediate waters preceded that of surface waters and atmosphere. Interstadial terminations are marked by rapid increases in benthic and planktonic $\delta^{18}O$ values, indicating cooling synchrony between surface and intermediate waters.

The benthic $\delta^{13}C$ record (*28*) exhibits large millennial-scale oscillations (up to 5‰) in concert with the D-O cycles (Figs. 2 and 3). In general, interstadial values are very negative (−2 to −6‰), while stadial values are more positive (~−1‰). Interstadials are associated with low-diversity benthic foraminiferal assemblages characteristic of low-oxygen environments and laminated sediments; stadials show higher diversity benthic foraminiferal assemblages indicative of well-oxygenated environments and nonlaminated sediments. Stadial-interstadial shifts in carbon isotopic composition occurred within decades to centuries, with higher isotopic variability recorded during interstadials. The early Holocene [10 to 7 thousand years ago (ka)] had very negative $\delta^{13}C$ values (up to −3.5‰, much like interstadials) compared with the middle Holocene (7 to 3 ka) (~−1‰) (Fig. 2). Carbon isotopic values decreased again (to ~−2.5‰) during the late Holocene. The benthic $\delta^{13}C$ record is punctuated by brief, negative excursions near the beginning of D-O 11 (~−5.5‰ at 44 ka) and during the early part of D-O 8 (~−6‰ at 37.5 ka) (Figs. 2 and 3). All species analyzed during these events exhibit very negative values although interspecies differences are apparent.

Planktonic $\delta^{13}C$ values (*28*) remained relatively unchanged during the last 60 ka except for several brief, negative excursions (Figs. 2 and 3). The most negative planktonic $\delta^{13}C$ shifts coincide with the benthic shifts near the beginnings of D-O 11 and 8 (Figs. 2 and 3). In D-O 11, the $\delta^{13}C$ shift (*Globigerina bulloides*, ~−3‰; *Neogloboquadrina pachyderma*, ~−2.5‰; *Globigerina quinqueloba*, ~−3.5‰) was followed ~200 years later by a second, smaller $\delta^{13}C$ shift (*G. bulloides* and *N. pachyderma*, ~−1.5‰; *G. quinqueloba*, ~−2.5‰). During D-O 8, the $\delta^{13}C$ shift (*G. bulloides* and *N. pachyderma*, ~−2.0‰; *G. quinqueloba*, ~−2.5‰; *Globorotalia scitula*, ~−1.5‰) were followed ~400 years later by a smaller shift (*G. bulloides*, ~−1.5‰; *N. pachyderma*, ~−0.5‰; *G. quinqueloba*, ~−1.5‰; *G. scitula*, ~−1.0‰). Two smaller $\delta^{13}C$ excursions of ~−1 to 1.5‰ occurred in planktonic species in D-O cycles 16/17 between 56 and 59 ka (Fig. 2). $\delta^{18}O$ values remained unchanged during the $\delta^{13}C$ shifts. We are confident in the veracity of these data because (i) the negative shifts were found in replicate analyses of samples and (ii) our examination of foraminiferal specimens by light and scanning electron microscopy found distinct primary surface ultrastructure present (*29*) and no evidence of diagenetic calcite overgrowths, thus demonstrating excellent preservation.

The benthic foraminiferal $\delta^{13}C$ time series (Figs. 2 and 3) was constructed using different taxa because benthic faunas are almost completely mutually exclusive between stadial and interstadial episodes (*30*). The highly negative $\delta^{13}C$ values of benthic foraminifera during interstadials and the large $\delta^{13}C$ changes between interstadial and stadial episodes (Figs. 2 and 3) could have resulted from interspecific (biological) fractionation differences (vital effects) (*31*), changes in pore water $\delta^{13}C$ composition in which the foraminifera lived (*32, 33*), or a combination of both. Strong $\delta^{13}C$ gradients can occur in the upper few cm of sediments below the sediment-water interface (*32*). It is difficult to separate the environmental and vital influences because little is known about the detailed ecology of the species analyzed here. Nevertheless, several lines of evidence suggest that the millennial-scale stadial-interstadial $\delta^{13}C$ oscillations during the late Quaternary (Figs. 2 and 3) largely reflect changes in the $\delta^{13}C$ of pore waters: First, the large $\delta^{13}C$ variability exhibited by individual species during interstadials (especially *Bolivina tumida*) (Figs. 2 and 3) are larger in magnitude than any suspected interspecific fractionation; second, the brief, large $\delta^{13}C$ excursions were recorded by every species analyzed during these events, demonstrating a response to environmental change rather than interspecies differences; third, interstadial species, known to be living near the sediment-water interface because of their occurrence in laminated sediments, record negative $\delta^{13}C$ pore water values equivalent to those that would have occurred at

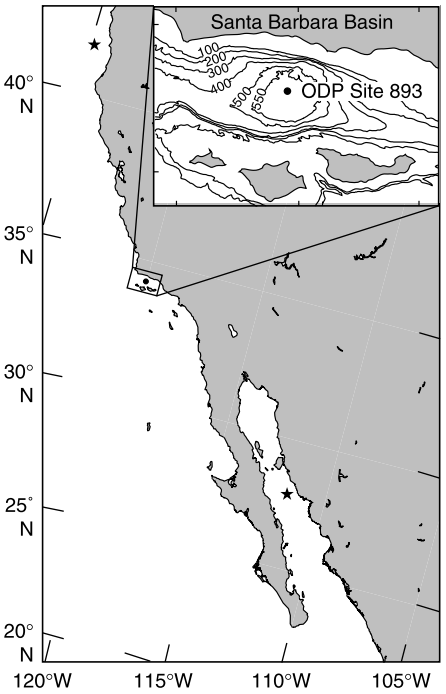

Fig. 1. Location of the Santa Barbara Basin and ODP Site 893 on the California margin. Gas hydrates are likely widespread along the margins of California and in the Gulf of California in association with a well-developed oxygen-minimum zone and have been reported off northern California (★, top of map) (*47*), the Santa Barbara Basin (*26*), and the Gulf of California (★, bottom of map) (*48*).

significant depths during stadials and the late Holocene. It is unlikely that a significant proportion of the abundant benthic foraminifera would have lived at such depths in the laminated sediment. Furthermore, because interstadial species lived in a low-oxygen benthic environment inhospitable to stadial taxa such as *Uvigerina* and *Rutherfordoides*, it is reasonable that they recorded pore water $\delta^{13}C$ values more negative than those ever recorded by stadial forms.

We therefore conclude that the highly negative $\delta^{13}C$ values during interstadials and the magnitude of stadial-interstadial $\delta^{13}C$ changes are too large to be explained by vital effects or foraminiferal vertical migration over large $\delta^{13}C$ gradients (*33*). Migration depths (10 to 20 cm) are too large and stadial-interstadial benthic faunas too different. It is also unlikely that benthic foraminifera lived in the sulfate reduction zone where the oxidation of organic matter significantly decreases the $\delta^{13}C$ of pore water CO_2 (*34*).

The very negative $\delta^{13}C$ values of interstadial benthic foraminifera most likely reflect presence of biogenic CH_4 in benthic microenvironments (*35*). As suggested for similar settings off Peru (*34*), oxidation of CH_4 in sediment pore spaces in the Santa Barbara Basin likely transferred a highly negative $\delta^{13}C$ signal to dissolved inorganic carbon (DIC). Presence of high CH_4 concentrations in the Santa Barbara Basin during inter-

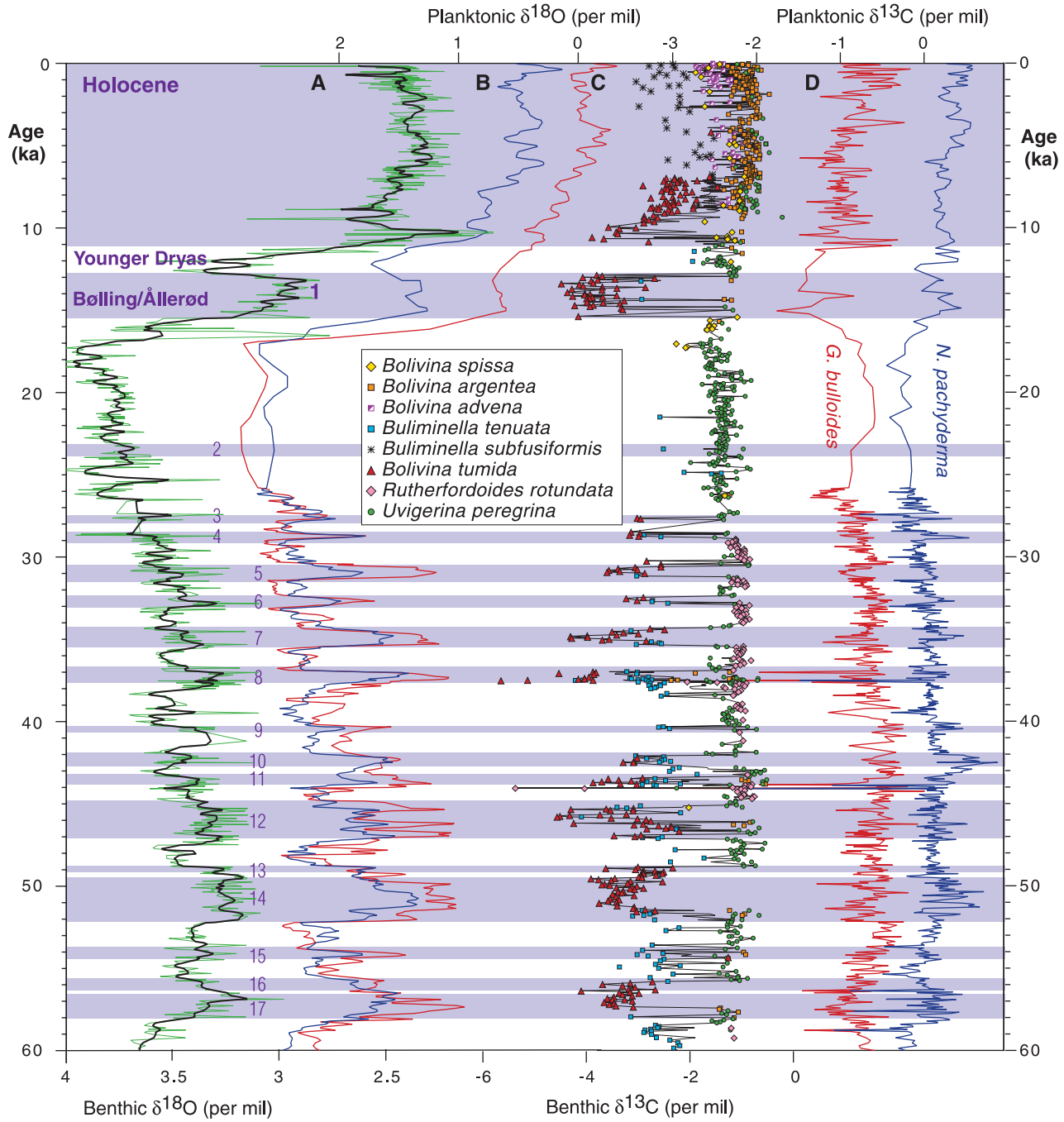

Fig. 2. Comparison of planktonic and benthic foraminiferal oxygen and carbon isotope records from ODP Site 893A, Santa Barbara Basin, for the last 60 ka. (**A**) Benthic $\delta^{18}O$ record (green) and five-channel binomial average (black). (**B**) Planktonic $\delta^{18}O$ record (*Neogloboquadrina pachyderma*, five-channel binomial smoothing) (*16, 17*). (**C**) Planktonic $\delta^{18}O$ record (*Globigerina bulloides*, five-channel binomial smoothing) (*16, 17*). (**D**) Benthic $\delta^{13}C$ record (species shown in box) and planktonic $\delta^{13}C$ records (*G. bulloides* and *N. pachyderma*). Shading represents laminated intervals (*15*) associated with warming (interstadials and Holocene). Interstadials are numbered. Time scale follows those of (*15–17*).

stadials is consistent with poor basin ventilation, low oxygen levels, low-diversity benthic foraminiferal assemblages, and the presence of sediment laminations. This interpretation suggests that *B. tumida* and *Buliminella tenuata*, which consistently exhibit the most negative $\delta^{13}C$ values, inhabited CH_4-rich environments, with *B. tumida* being the most sensitive indicator of CH_4. *Bolivina tumida* disappeared from the Site 893A faunal record at ~7 ka, but has been found closely associated with modern methane seeps in the basin (*36*).

Changes in $\delta^{13}C$ composition differ between species from stadial to interstadial (Fig. 3), as does relative faunal abundance. These changes appear to reflect both varying sensitivity to CH_4 (*34*), and at other times, foraminiferal depth habitat in the $\delta^{13}C$ gradient (*33*). Interstadials are marked by a sequential change in fauna (*19*) and isotopic composition, marked initially by increased abundance of *B. tenuata* and slightly more negative $\delta^{13}C$ values (0.5‰), followed by high abundance of *B. tumida* and its highly negative $\delta^{13}C$ values. This sequence likely signifies decreasing organic matter oxidation associated with increased CH_4 concentrations in surface sediments.

The basin $\delta^{13}C$ record reflects two different but interrelated processes associated with stadial-interstadial climate oscillation: (i) millennial-scale change in vertical CH_4 flux through basin sediments as recorded in benthic foraminiferal $\delta^{13}C$ values and possibly faunal composition; (ii) massive, episodic release of CH_4 from basin sediments on decadal time scales, due to localized deroofing of gas hydrates. These brief episodes are recorded as large negative $\delta^{13}C$ excursions in both benthic and planktonic forms.

We suggest that stadial-interstadial benthic $\delta^{13}C$ oscillations reflect extreme benthic environmental changes (*32–34*) best explained by vertically migrating sedimentary CH_4 gradients (Fig. 4). Stadial-interstadial vertical migration of the CH_4 gradient within the near-surface sediment layer would effect DIC $\delta^{13}C$ values. In the modern basin, the CH_4 zone lies below ~1 m of sediment (*37*), with very low concentrations of CH_4 above, reflecting consumption of upwardly diffusing CH_4 by bacteria in the sulfate-reducing zone (*37*). During the late Holocene and cool periods of the late Quaternary (Younger Dryas, Last Glacial Maximum, and stadials of marine isotope stage 3) the CH_4 zone likely occurred at depths below the benthic foraminiferal habitat (Fig. 4D). We suggest that during interstadials, the CH_4 zone migrated close to the sediment-water interface, allowing CH_4 diffusion to overwhelm bacterial consumption (Fig. 4, A and B) (*38*). Despite low flux rates from the sediment, CH_4 concentrations are currently high in basin bottom waters (*39*), but are greatly reduced by oxidation within 100 m above the sea floor (*39*). Although increased CH_4 flux into the water column resulted from interstadial conditions, absence of negative planktonic $\delta^{13}C$ oscillations in concert with D-O cycles (Fig. 2) indicates that typical diffusion from sediments was insufficient to affect surface-water $\delta^{13}C$ values.

Changes in the upward flux and vertical sedimentary gradient of CH_4 during D-O cycles reflect modulation of gas hydrate stability by bottom-water temperature oscillations of 2° to 3.5°C (Fig. 4) (*20*). Increased upward diffusion of CH_4 during interstadials is likely to have resulted from dissociation of gas hydrates at depth (Fig. 4, A and B) (*38*), which are sensitive to changes in temperature of only 1° to 2°C (*40*) and/or of pressure (*9*). Thus, periodic upward diffusion of CH_4 occurred when bottom waters were relatively warm during interstadials (Fig. 4, A and B), and ceased during stadials when bottom waters were cooler (Fig. 4, C and D). This model also explains the Holocene benthic $\delta^{13}C$ record of Hole 893A (Fig. 2), because reduced fluxes of CH_4 after 7 ka would have resulted from increased stability of gas hydrates as sea level rose and bottom-water temperatures stabilized. This stability increase is supported by the *B. tumida* $\delta^{13}C$ record which exhibits increasingly positive $\delta^{13}C$ values following the Younger Dryas (Fig. 2) until disappearing from the basin at 7 ka.

Massive, brief, probably localized releases of CH_4 from basin sediments (Fig. 4A) are inferred from the large negative $\delta^{13}C$ excursions (−2.5 to −4‰) exhibited by planktonic and benthic foraminifera during D-O 11 and 8 (Figs. 2 and 3). These shifts are present in up to three sequential samples (Fig. 3), each representing <20 years duration and are recorded by species living at different water depths (Fig. 3), as well as by benthic taxa (with slightly larger negative shifts of up to 4.5‰).

These results suggest that for brief episodes, the $\delta^{13}C$ values of inorganic carbon became very negative at all water depths in Santa Barbara Basin (~500 m during marine isotope stage 3). This scenario is best explained by release of large volumes of sedimentary CH_4 into the water column as a result of sediment slope failure in Santa Barbara Basin deroofing gas hydrates (*26*) and releasing free gas into the water column (Fig. 4A). Similar negative $\delta^{13}C$ shifts (<3‰) contemporaneously recorded by several planktonic species in late Quaternary sediments of the Amazon fan have been attributed to massive local CH_4 releases to surface waters, following sediment failure and deroofing of gas hydrates (*13*). $\delta^{13}C$ excursions of ~–3‰ in marine carbonate, close to values documented here, have been calculated to result from massive releases of CH_4 (*41*).

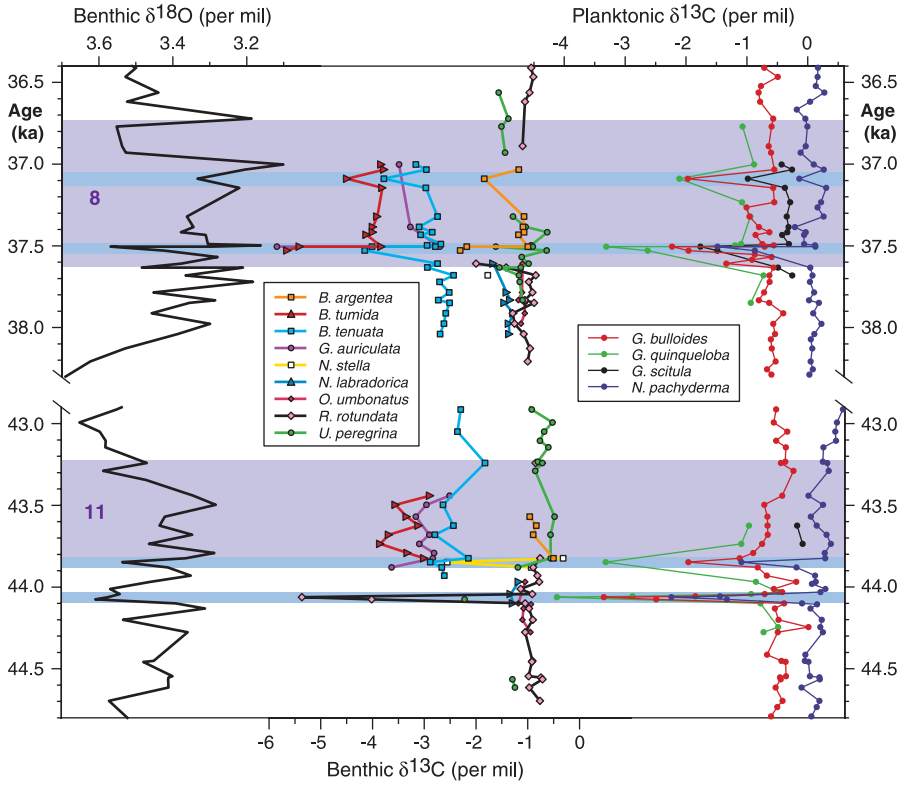

Fig. 3. Detailed comparison of benthic $\delta^{18}O$, benthic $\delta^{13}C$, and planktonic $\delta^{13}C$ records during D-O 8 and 11 from ODP Site 893A. Species analyzed are shown in boxes. Purple shading represents laminated intervals, and blue highlights indicate negative $\delta^{13}C$ excursions.

Massive releases of CH_4 by dissociation of basinal gas hydrates requires either increased bottom-water temperature and/or decreased pressure through falling sea level. Present-day water depths (580 m) and bottom-water temperatures (~5.5°C) in the basin are close to the phase change between hydrate and free gas (*8*). Stadial-interstadial bottom-water temperature shifts of 2° to 3.5°C (*20*) were sufficiently large to form/dissociate gas hydrates in basin sediments and over broad regions of the circum north Pacific that felt the affects of the thermohaline switching (*20*). Dissociation of gas hydrates most likely occurred near the beginning of interstadials, when the largest negative planktonic $\delta^{13}C$ excursions (Figs. 2 and 3) occurred, because bottom waters warmed while sea level was ~80 m lower than present contributing to higher instability (*42*). The CH_4 was most likely derived from an intrabasinal source for benthic foraminifera to record the large negative signals. Smaller negative planktonic $\delta^{13}C$ excursions near D-O 17 are not recorded by benthic foraminifera and may reflect advection of CH_4-rich surface waters into the basin.

A minimum estimate of the amount of CH_4 released from sediments required to account for the large negative $\delta^{13}C$ excursions can be calculated (*43*). Assuming an instantaneous exchange of carbon between the CH_4 and DIC, 1.9×10^9 m^3 of CH_4 would have been oxidized in the water column. This is equivalent to 1.3 Tg which amounts to ~0.2% of the total modern annual flux to the atmosphere (~510 Tg) (*44*) or ~0.2% of the typical increase associated with interstadials (*45*). However, this estimate does not take into account the event's possible duration based on core chronology and the residence time of basin surface waters. Including this significantly increases the inferred volume of CH_4 release: 1.3×10^{11} m^3 of CH_4 oxidized in the water column equivalent to 90 Tg of CH_4. This represents an annual flux of 6.4 Tg, equal to ~1.3% of the modern annual flux. The total release over the duration of the event was ~18% of the average CH_4 increase associated with interstadials. It is likely that the total amount of CH_4 released into the water and atmosphere during such events exceeded this value because the amount that escaped directly into the atmosphere has not been taken into account.

The Santa Barbara Basin sequence records at least four episodes of brief, massive release of CH_4 from continental margin sediments, resulting in negative $\delta^{13}C$ shifts throughout the entire water column, but given their brevity, others may have occurred but remain undetected. Such releases are inferred to have resulted from deroofing of gas hydrates due to sediment failure caused by gas hydrate dissociation associated with millennial-scale bottom-water temperature changes. These brief, catastrophic events are superimposed on longer stadial-interstadial oscillations in benthic foraminiferal $\delta^{13}C$ values consistent with the modulation of CH_4 flux through sediments by intermediate water temperature changes. Both of these processes may have been widespread on continental margins in the past, and support mounting geologic evidence for past pervasive, massive CH_4 releases from the marine sediment reservoir (*12*). This work lends support to the hypothesis that CH_4 venting into the atmosphere from gas hydrates contributed to increased atmospheric CH_4 during latest Quaternary interstadials (*46*).

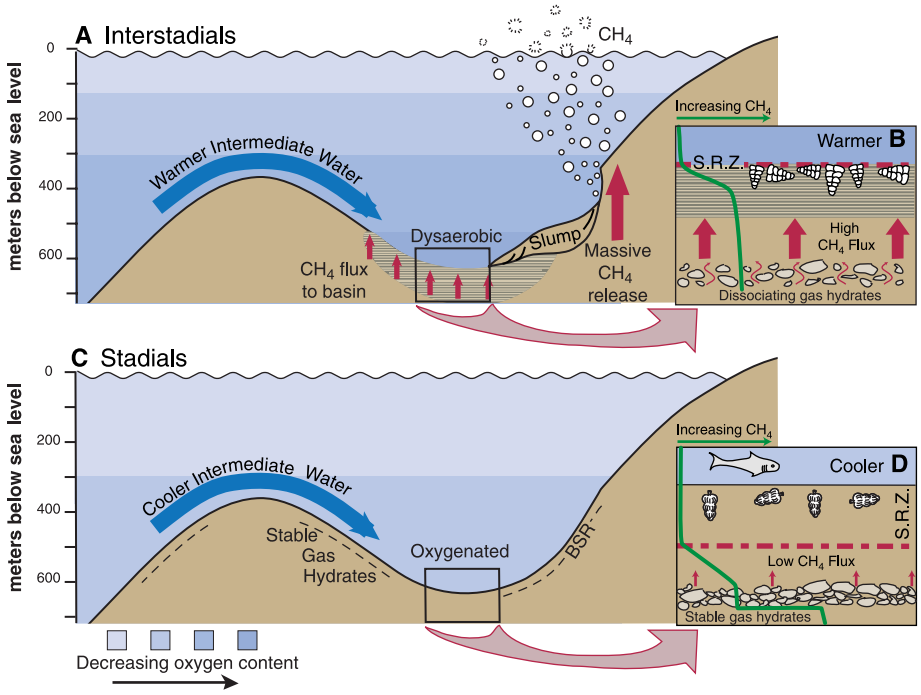

Fig. 4. Schematic diagram illustrating stadial-interstadial modes of CH_4 flux for Santa Barbara Basin. (**A** and **B**) During interstadials, warmer intermediate waters destabilized gas hydrates and activated CH_4 flux through basin sediments. This led to increased upward CH_4 flux through surface sediments to basin bottom waters. Episodic deroofing of gas hydrates caused massive CH_4 releases into water column and atmosphere [bubbles in (A)]. (**C** and **D**) During stadials, cooler intermediate waters lead to gas hydrate stability and build-up, an expanded sulfate reduction zone (S.R.Z.), and reduced upward CH_4 flux into basin. Green line in (B) and (D) represents inferred CH_4 gradient within sediments. Changing flux rates through basin sediments are reflected by the $\delta^{13}C$ of benthic foraminifera and faunal composition of assemblages living in surface and near-surface sediments (A, B, and D). BSRs are bottom-simulating reflectors inferred to represent gas accumulations beneath gas hydrates.

References and Notes

1. C. Lorius *et al.*, *Nature* **347**, 139 (1990); J. Chappellaz *et al.*, *Nature* **345**, 127 (1990); E. J. Brook, T. Sowers, J. Orchardo, *Science* **273**, 1087 (1996).
2. D. Raynaud, J. Chappellaz, T. Blünier, *Geol. Soc. Spec. Publ.* **137**, 327 (1998).
3. J. P. Severinghaus *et al.*, *Nature* **391**, 141 (1998).
4. M. L. Salgado-Labouriau *et al.*, *Rev. Palaeobot. Palynol.* **99**, 115 (1998); M.-P. Ledru, M. L. Salgado-Labouriau, M. L. Lorscheitter, *Rev. Palaeobot. Palynol.* **99**, 131 (1998); H. Behling and H. Hooghiemstra, *J. Paleolimnol.* **21**, 461 (1999); K. Liu and H. Qiu, *Terrest. Atmos. Oceanic Sci.* **5**, 393 (1994); M. G. Bonnefille and F. Chalié, *Global Planet. Changes*, in press; M. G. Winkler, P. R. Sanford, S. W. Kaplan, *Bull. Am. Paleontol.*, in press.
5. K. A. Kvenvolden, *Global Biogeochem. Cycles* **2**, 221 (1988); C. K. Paull *et al.*, *Geology* **24**, 143 (1996).
6. K. A. Kvenvolden, *Chem. Geol.* **71**, 41 (1988); G. T. MacDonald, *Annu. Rev. Energy* **15**, 5 (1990); G. R. Dickens *et al.*, *Nature* **385**, 426 (1997).
7. K. A. Kvenvolden, *Org. Geochem.* **23**, 997 (1995); R. J. Cicerone and R. S. Oremland, *Global Biogeochem. Cycles* **2**, 299 (1988).
8. G. R. Dickens and M. S. Quinby-Hunt, *Geophys. Res. Lett.* **21**, 2115 (1994); P. G. Brewer *et al.*, *Geology* **25**, 407 (1997).
9. C. K. Paull and W. Ussler III, *Geophys. Res. Lett.* **18**, 432 (1991); B. U. Haq, *Geol. Soc. Spec. Publ.* **137**, 303 (1998).
10. G. R. Dickens *et al.*, *Paleoceanography* **10**, 965 (1995); M. E. Katz *et al.*, *Science* **286**, 1531 (1999).
11. I. R. MacDonald *et al.*, *Geology* **22**, 699 (1994).
12. R. E. Kayen and H. J. Lee, *Mar. Geotechnol.* **10**, 125 (1991); E. G. Nisbet, *J. Geophys. Res.* **97**, 12859 (1992); D. Evans *et al.*, *Mar. Geol.* **130**, 281 (1996); E. G. Nisbet and D. J. W. Piper, *Nature* **392**, 329 (1998); M. Maslin *et al.*, in *Proc. Ocean Drill. Program Sci. Results* **155** (Ocean Drilling Program, College Station, TX, 1998), pp. 305–318; R. G. Rothwell, J. Thomson, G. Kähler, *Nature* **392**, 377 (1998).
13. M. Maslin *et al.*, *Geology* **26**, 1107 (1998).
14. W. S. Reeburgh, S. C. Whalen, M. J. Alperin, in *Microbial Growth on C_1 Compounds*, J. C. Murrell and D. P. Kelly, Eds. (Intercept, Andover, UK, 1993), pp. 1–14.
15. R. J. Behl and J. P. Kennett, *Nature* **379**, 243 (1996).
16. J. P. Kennett and B. L. Ingram, *Nature* **377**, 510 (1995).
17. I. L. Hendy and J. P. Kennett, *Geology* **27**, 291 (1999); J. P. Kennett *et al.*, *Ocean Drill. Program*, Leg 167 (Ocean Drilling Program, College Station, TX), in press.

18. W. Dansgaard *et al.*, *Nature* **364**, 218 (1993); S. J. Johnsen *et al.*, *Nature* **359**, 311 (1992).
19. K. G. Cannariato and J. P. Kennett, *Geology* **27**, 975 (1999); K. G. Cannariato, J. P. Kennett, R. J. Behl, *Geology* **27**, 63 (1999).
20. I. L. Hendy and J. P. Kennett, in preparation.
21. A. Van Geen *et al.*, *Paleoceanography* **11**, 519 (1996).
22. Samples (2 cm thick, averaging 14 years) were taken every 5 to 7 cm (50 to 70 years). Sampling resolution is lower between 13 and 25 ka. From 8 to 40 planktonic and 5 to 10 benthic foraminifera were picked from each sample for analysis using a Finnigan/MAT 251 light stable isotope mass spectrometer and standard preparation techniques. Instrumental precision is <0.09‰ for both isotopes, with all data expressed as standard δ notation in ‰ relative to the Pee Dee Belemnite, related by repeated analysis to NBS-19 and NBS-20. The chronology is based on 17 accelerator mass spectrometry radiocarbon dates and three SPECMAP datums (*15–17*), as the ODP Hole 893A benthic foraminiferal $\delta^{18}O$ record correlates well with the standard late Quaternary $\delta^{18}O$ stratigraphy.
23. J. P. Kennett *et al.*, Eds., *Proc. Ocean Drill. Program Initial Reports* **146** (part 2) (Ocean Drilling Program, College Station, TX, 1994); J. P. Kennett *et al.*, Eds., *Proc. Ocean Drill. Program Sci. Results* **146** (part 2) (Ocean Drilling Program, College Station, TX, 1994).
24. Properties of kerogen in Hole 893A suggest an episodic recycling of CH_4 in basin sediments [L. M. Pratt, A. M. Carmo, V. Brüchert, S. M. Monk, J. M. Hayes, in J. P. Kennett *et al.*, Eds., *Proc. Ocean Drill. Program Sci. Results* **146** (part 2) (Ocean Drilling Program, College Station, TX, 1994), pp. 213–218].
25. J. W. Yun, D. L. Orange, M. E. Field, *Mar. Geol.* **154**, 357 (1999).
26. J. P. Kennett and C. C. Sorlien, *AAPG Bull.* **83**, 692 (1998).
27. I. L. Hendy and J. P. Kennett, *Paleoceanography* **15**, 30 (2000).
28. The benthic $\delta^{13}C$ record is based on several species since no benthic species ranges throughout the sequence because of extreme changes in basin oxygenation associated with D-O cycles. Overlap of a few species allows interspecies $\delta^{13}C$ stadial-interstadial comparisons. For interstadials, we analyzed *Bolivina argentea*, *Bolivina tumida*, *Buliminella tenuata*, and *Bolivina spissa*; for stadials, we analyzed *Uvigerina peregrina* and *Rutherfordoides rotundata*. For short key intervals, we also analyzed *Globobulimina auriculata*, *Buliminella subfusiformis*, and *Bolivina advena*. We produced complete $\delta^{13}C$ records of *Globigerina bulloides* (surface water) and *Neogloboquadrina pachyderma* (thermocline) [D. Pak, J. P. Kennett, M. Kashgarian, *Eos* **78**, 359 (1997)] and short records of *Globigerina quinqueloba* (surface water) and *Globorotalia scitula* (subthermocline) [J. D. Ortiz, A. C. Mix, R. W. Collier, *Paleoceanography* **10**, 987 (1995); J. D. Ortiz *et al.*, *Geochim. Cosmochim. Acta* **60**, 4509 (1996)].
29. J. P. Kennett and M. S. Srinivasan, *Neogene Planktonic Foraminifera: A Phylogenetic Atlas* (Hutchinson Ross, Stroudsburg, PA, 1983).
30. Overlapping taxonomic ranges between stadials and interstadials at some levels are reflected only by rare specimens that may be environmentally unrepresentative of that climatic episode.
31. W. H. Berger and E. Vincent, *Geol. Rundsch.* **75**, 249 (1986).
32. D. C. McCorkle and S. R. Emerson, *Geochim. Cosmochim. Acta* **52**, 1169 (1988); D. C. McCorkle and G. P. Klinkhammer, *Geochim. Cosmochim. Acta* **55**, 161 (1991); J. M. Bernhard, B. K. Sen Gupta, P. F. Borne, *J. Foram. Res.* **27**, 301 (1997).
33. R. Zahn, K. Winn, M. Sarnthein, *Paleoceanography* **1**, 27 (1986); D. C. McCorkle *et al.*, *Paleoceanography* **5**, 161 (1990); G. J. Van der Zwaan *et al.*, *Earth Sci. Rev.* **46**, 213 (1999).
34. G. Wefer, P. M. Heinze, W. H. Berger, *Nature* **369**, 282 (1994).
35. Within the ocean, oxidation of CH_4 to CO_2 is carried out by methanotrophic bacteria (*5*), which decreases DIC $\delta^{13}C$ values. Bicarbonate ion incorporation during shell growth transfers the negative $\delta^{13}C$ value to foraminiferal $CaCO_3$. Negative $\delta^{13}C$ values may also be taken up by foraminifera through consumption of methanotrophic bacteria.
36. J. P. Kennett, unpublished data.
37. R. O. Barnes and E. E. Goldberg, *Geology* **4**, 297 (1976); A. L. Warford, D. R. Kosiur, P. R. Doose, *Geomicrobiol. J.* **1**, 117 (1979).
38. W. S. Borowski, C. K. Paull, W. Ussler III, *Geology* **24**, 655 (1996).
39. F. J. Cynar and A. A. Yayanos, *J. Geophys. Res.* **97**, 11269 (1992).
40. V. Gornitz and I. Fung, *Global Biogeochem. Cycles* **8**, 335 (1994).
41. Y. Zhang, personal communication.
42. J. Chappell *et al.*, *Earth Planet. Sci. Lett.* **141**, 227 (1996).
43. The amount of CH_4 responsible for changing the $\delta^{13}C$ of DIC of entire water column (~500 m) by ~3‰ (the average foraminiferal isotopic change during the 44.1-ka excursion) can be calculated from this relationship: $\delta^{13}C_{CH4}(C_{CH4}) + \delta^{13}C_{DIC\ before}(C_{DIC\ before}) = \delta_{13}C_{DIC\ after}(C_{DIC\ after})$. The calculation for instantaneous carbon transfer assumes basin volume of 850 km^3; methane $\delta^{13}C$ of −65‰; and DIC of 2000 μmol/kg. The time-dependent calculation assumes an event duration of 14 years; residence time of surface waters in Santa Barbara Channel of 30 days. We infer a longer residence time compared with the present day (~10 days) [M. C. Henderscott, *Fifth California Islands Symposium*, 29 March to 1 April 1999, Santa Barbara, p. 21; S. Harms and C. D. Winant, *J. Geophys. Res.* **103**, 3041 (1998)] because of the location of Site 893A near the center of the basin gyre.
44. M. A. K. Khalil and R. A. Rasmussen, in *Composition, Chemistry, and Climate of the Atmosphere*, H. B. Singh, Ed. (Van Nostrand Reinhold, New York, 1995), pp. 50–87.
45. R. Stauffer *et al.*, *Nature* **392**, 59 (1998).
46. E. G. Nisbet, *Can. J. Earth Sci.* **27**, 148 (1990).
47. M. E. Field and K. A. Kvenvolden, *Geology* **13**, 517 (1985); J. M. Brooks, M. E. Field, M. C. Kennicutt II, *Mar. Geol.* **96**, 103 (1991); P. G. Brewer *et al.*, *Eos* **78**, 340 (1997)
48. P. Lonsdale, *AAPG Bull.* **69**, 1160 (1985).

49. We thank personnel of the Ocean Drilling Program for their efforts during drilling and assistance with sampling. We also thank D. Krause for encouragement and enlightening discussions during this work and for review of the manuscript. Critical inspiration came from the work of E. Nisbet and G. Dickens. We thank two anonymous reviewers for constructive advice. Careful technical assistance was provided by K. Thompson and H. Berg. Supported by NSF grant EAR99-0424 (Earth System History) and an NSF Fellowship to I.L.H. Twenty-five percent of this research was funded by the National Institute for Global Environmental Change through the U.S. Department of Energy (DOE) (Cooperative Agreement DE-FC03-90ER61010). Conclusions expressed in this publication are those of the authors and do not necessarily reflect the views of the DOE.

18 October 1999; accepted 23 February 2000

Sink or Swim: Strategies for Cost-Efficient Diving by Marine Mammals

Terrie M. Williams,[1]* R. W. Davis,[2] L. A. Fuiman,[3] J. Francis,[4] B. J. Le Boeuf,[1] M. Horning,[2] J. Calambokidis,[5] D. A. Croll[6]

Locomotor activity by diving marine mammals is accomplished while breath-holding and often exceeds predicted aerobic capacities. Video sequences of freely diving seals and whales wearing submersible cameras reveal a behavioral strategy that improves energetic efficiency in these animals. Prolonged gliding (greater than 78% descent duration) occurred during dives exceeding 80 meters in depth. Gliding was attributed to buoyancy changes with lung compression at depth. By modifying locomotor patterns to take advantage of these physical changes, Weddell seals realized a 9.2 to 59.6% reduction in diving energetic costs. This energy-conserving strategy allows marine mammals to increase aerobic dive duration and achieve remarkable depths despite limited oxygen availability when submerged.

Swimming is energetically expensive for mammals and results in transport costs that are 2 to 23 times the levels predicted for fish (*1, 2*). To reduce these costs, marine mammals have developed a wide variety of energy-conserving swimming behaviors. Adherence to a narrow range of routine transit speeds (*3, 4*), wave-riding (*5*), and porpoising (*6*) decrease the amount of energy expended when pinnipeds and cetaceans move near the water surface. Although these energy-conserving strategies are especially beneficial during underwater activity, when access to ambient oxygen is limited, two of the behaviors, porpoising and wave-riding, cannot be used when the animal is submerged. In view of this, it has been assumed that marine mammals swim constantly at cost-efficient routine speeds during diving (*3, 4*). Indeed, the routine speeds of many freely diving marine mammals fall within a relatively narrow range (*7, 8*). A paradox arises when

[1]Department of Biology, EMS-A316, University of California, Santa Cruz, CA 95064, USA. [2]Department of Marine Biology, Texas A&M University, 5007 Avenue U, Galveston, TX 77553, USA. [3]Department of Marine Science, University of Texas at Austin, 750 Channel View Drive, Port Aransas, TX 78373, USA. [4]Committee for Research and Exploration, National Geographic Society, 1145 17th Street NW, Washington, DC 20036, USA. [5]Cascadia Research, 218½ West Fourth Avenue, Olympia, WA 98501, USA. [6]Institute of Marine Science, EMS-A316, University of California, Santa Cruz, CA 95064, USA.

*To whom correspondence should be addressed. E-mail: williams@darwin.ucsc.edu